Physica B: Condensed Matter 559 (2019) 62–65

Contents lists available at ScienceDirect

Physica B: Condensed Matter

journal homepage: www.elsevier.com/locate/physb

X-ray excited optical luminescence and morphological studies of Eu-doped $LiAl_5O_8$

Verônica C. Teixeira[a], Adriano B. Andrade[b], Nilson S. Ferreira[b,c], Douglas Galante[a], Lucas C.V. Rodrigues[d], Marcos V.dos S. Rezende[e,*]

[a] Laboratório Nacional de Luz Síncrotron (LNLS), Centro Nacional de Pesquisa em Energia e Materiais (CNPEM), CEP, 13084-971, Campinas, SP, Brazil
[b] Departamento de Física, Universidade Federal de Sergipe, 49100-000, São Cristóvão, SE, Brazil
[c] PPGCA, Universidade Federal do Amapá, 68902-280, Macapá, AP, Brazil
[d] Departamento de Química Fundamental, Instituto de Química, Universidade de São Paulo, 05508-000, São Paulo, SP, Brazil
[e] Grupo de Nanomateriais Funcionais (GNF), Departamento de Física, Universidade Federal de Sergipe, 49500-000, Itabaiana, SE, Brazil

ARTICLE INFO

Keywords:
Lithium aluminates
Europium
XEOL

ABSTRACT

This work aims the investigation of lithium excess influence on the X-ray Excited Optical Luminescence (XEOL) and X-ray Absorption Spectroscopy (XAS) of Eu-doped $LiAl_5O_8$ samples. XEOL spectra excited at Eu L_{III}-edge is composed of emission peaks attributed to the emission of Eu^{2+}, Eu^{3+} and Cr^{3+} ions. The results showed that lithium excess contributes to important differences concerning the relative intensity of Eu^{2+} and Eu^{3+} emissions, suggesting that can Li^+ or Li vacancies act to create defects able to stabilize the Eu^{2+} on the host lattice. Scanning electronic microscopy images showed that the Li^+ excess did not contribute to significant changes on the particles' morphology and size. Based on the XAS measurements, we suggest that defects such as V'_{Li} may be created in the $LiAl_5O_8$ structure contributing to the Eu^{2+} stabilization. Consequently, the Li^+ excess favors the Eu^{3+} stabilization and the preparation of red emitting phosphors.

1. Introduction

Lithium aluminate ($LiAl_5O_8$) is an attractive host to produce luminescent materials. Its structure is an inverse spinel-type that has been doped with rare earth and transition metal ions for different purposes, such as phosphors for plasma-panel displays, temperature sensors, cathode for X-ray tubes, light emitting diodes, electroluminescence panels, etc. [1–4].

Several studies have demonstrated that the luminescence yield of rare earth-doped phosphors may be enhanced by tuning the symmetry of the crystal field around optically active ions. Thus, different conditions such as annealing temperatures, structural composition and particle size and morphology have been controlled to get improved optical properties for specific applications [5–7]. Some studies have reported also that the addition of Li^+ may improve the luminescence yield due the ability of these ions promoting changes around the optically active ion. For some phosphors, Li^+ ions play roles such as flux [8] and also create oxygen vacancies [9], which may strongly influence the material optical properties.

In our previous work [10], we have demonstrated the optical behavior of a Eu-doped $LiAl_5O_8$ host with Li excess under excitation in the vacuum ultraviolet and tender X-ray range (Al K-edge). In this work, we discuss the Eu valence through X-ray absorption near-edge structure, the morphology and the optical properties under hard X-ray excitation for Eu-doped $LiAl_5O_8$ samples (stoinchiometric and with Li^+ excess) thermally treated in two different temperatures (900 and 1000 °C).

2. Methodology

The samples were prepared using the sol-gel method based on polyvinyl alcohol (PVA),as demonstrated in previous work [10]. In this work, we focus on the study of $LiAl_5O_8$: 3mol%Eu and $Li_{1.05}Al_5O_8$: 3mol %Eu particles' morphology through scanning electron microscopy (SEM), optical properties under X-ray irradiation (X-ray Excited Optical Luminescence – XEOL) and the Eu oxidation state using the X-ray Absorption Near-Edge Structure (XANES) around the Eu - L_{III} edge (6977 eV). The samples were named $LiAl_5O_8$ for the one doped with 3 mol% of Eu and $Li_{1.05}Al_5O_8$ for samples doped with 3 mol% Eu and with 5 mol% of Li^+ excess. The samples, in both preparations, were calcined at 900 and 1000 °C for 2 h in static air atmosphere.

SEM images were recorded using a FEI Quanta 650 FEG available at the Brazilian Nanotechnology Laboratory (LNNano/CNPEM), in

* Corresponding author.
E-mail address: mvsrezende@gmail.com (M.V.d.S. Rezende).

https://doi.org/10.1016/j.physb.2019.01.050
Received 10 November 2018; Received in revised form 28 January 2019; Accepted 30 January 2019
Available online 01 February 2019

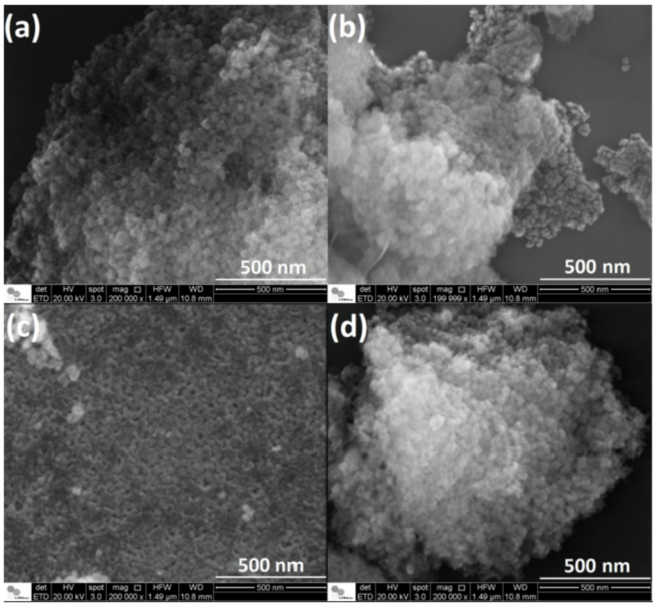

Fig. 1. SEM images of (a) $LiAl_5O_8$ 1000 °C, (b) $LiAl_5O_8$ 900 °C, (c) $Li_{1.05}Al_5O_8$ 1000 °C and (d) $Li_{1.05}Al_5O_8$ 900 °C.

secondary electrons mode with an Everhart-Thornley detector. Samples were dispersed in isopropanol (0.1 g/l) in ultrasonic bath during 10 min. A single drop collected at the dispersion half height was collected and deposited on oriented siliconchip [1 0 0]. The images were acquired with accelerating tension of 20 kV.

XEOL and XANES spectra were acquired at the X-ray Absorption and Fluorescence Spectroscopy beamline (XAFS2) [11] at the Brazilian Synchrotron Light Laboratory (LNLS/CNPEM) at room temperature. For both experiments, the samples were pressed in 13 mm diameter pellets. XEOL spectra were collected in emission mode in a dark chamber, coupled by an optical fiber to a spectrometer HR2000 from Ocean Optics. XANES spectra were acquired in fluorescence mode with a Ge15 detector from Canberra.

3. Results

As it was pointed out previously [10], the thermal treatment and the Li excess did not influence the crystalline phase of $LiAl_5O_8$. The particles morphology did not exhibit changes as well, as can be evaluated through SEM images showed in Fig. 1.

The images showed that all samples present similar morphological behavior. Particles present grain size in nanometric order and the formation of micrometric agglomerates independent of the synthesis condition. The nanometric scale-size of particles is associated with the presence of PVA in the synthesis starting reaction, in which, metal nitrates were dissolved and mixed with PVA solution. The PVA role is increase the metals ions homogenization on the colloidal solution through their complexation by the coordinating groups, such as hydroxyl, until the gel formation. After the burning process, the ceramic bottom-up grown process is favored [12–14] and the lithium aluminate materials were obtained.

The average particle size was calculated from the histograms presented in Fig. 2, in which 100 isolated particles from each sample were measured using the software ImageJ [15]. The particle size ranges from 10 to 35 nm in Gaussian distribution and the particle shape presents a spherical tendency, qualitative regular distribution and high agglomeration degree. It is a common effect observed on nanoparticles, due to the their high surface reactivity, which minimizes the interface strain energy [16,17]. This behavior is also observed for $LiAl_5O_8$ obtained through the self-propagating combustion method as shown by Singh and Rao [18].

The nanometric size and agglomeration degree may strongly influence the optical properties mainly due the surface effects and the high ratio particle surface/volume, which can induce changes on the stabilization of doping-ion oxidation state and on the crystalline field intensity around the material optical channels [19]. At this work, no strong difference was observed for the particles morphology, shape and agglomeration degree, even for samples calcined at different temperatures. But, we could observe the employed synthesis methodology is reliable to produce nanoparticles, which is an important criterion for the phosphors applications.

To observe the synthesis influence on the samples optical properties, the $LiAl_5O_8$ and $Li_{1.05}Al_5O_8$ emission spectra under hard X-ray irradiation was recorded at the Eu L_{III}-edge. It exhibited Eu^{2+}, Eu^{3+} and Cr^{3+} emissions as shown in Fig. 3.

The emission broad bands and lines are assigned to the Eu^{2+} $4f^65d^1 \rightarrow 4f^7$ (400–600 nm), Eu^{3+} $^5D_0 \rightarrow {}^7F_{0\text{-}4}$ (580–700 nm) and Cr^{3+} $^2E_g \rightarrow {}^4A_{2g}$ (730 nm). The chromium emission is associated with contamination from the Al precursor as was pointed out in our previous work [10]. This ion is optically active in the $LiAl_5O_8$ structure, resulting in an efficient emission, even when in very small amounts in this spinel host. The Eu^{2+}/Eu^{3+} valence mixture may come from the radiation exposure [20], thermal treatment [21] or the geometry around the ion [19]. Based on the third condition, we believe that due to the volatility of Li_2O during the synthesis process, defects such as V'_{Li} may be created in the $LiAl_5O_8$ structure favoring the stabilization of Eu^{2+}, which may be less energetic to complete the charge compensation, when compared to the insertion of Eu^{3+} in Li^+ sites. This conclusion is coherent with both the higher calcination temperature and the intensity of Eu^{2+} bands observed for the Eu-doped $LiAl_5O_8$ (1000 °C), when compared with $Li_{1.05}Al_5O_8$ (900 °C). The more V'_{Li} present, the more Eu^{2+} there is in the material, consequently, it is possible to observe a more intense band attributed to the Eu^{2+} on $LiAl_5O_8$ (1000 °C). On the other hand, Li excess produced less V'_{Li}, which disfavors the stabilization of Eu^{2+} ions, consequently, it is possible to observe a more intense band attributed to the Eu^{2+} on $LiAl_5O_8$ than on the $Li_{1.05}Al_5O_8$ samples. Thus, the Li^+ presence can be used to stabilize the Eu in the 3 + oxidizing state and producing red emitter phosphors based on nanometric lithium aluminates.

XANES measurements around the Eu-L_{III} edge were carried out to identify the most abundant Eu valence in the oxides. The data are presented in Fig. 4.

As can be observed in Fig. 4, the most abundant species in the lithium aluminates samples is the Eu^{3+} (edge position 6980 eV). The Eu-doped $LiAl_5O_8$ and $Li_{1.05}Al_5O_8$ absorption curves were compared to the Eu_2O_3-standard (99.99%, Sigma-Aldrich), in which Eu is purely in the trivalent form. The edge absorption position at 6980 eV, as showed in the derivative curves (inset of Fig. 3), suggests the prevalence of Eu^{3+} for all the samples. However, a very small shoulder at 6974 eV also suggests a little presence of Eu^{2+} in the lithium aluminates. It means that Eu^{2+} and Eu^{3+} co-exist in all prepared materials, as was observed via XEOL emission spectra (see Fig. 3). The amount of Eu^{2+} in each sample is similar among them, according to the band intensity between 6970 and 6977 eV. The slight difference among the areas under the peak with a maximum of 6974 eV is responsible for the Eu^{2+} $4f^65d^1 \rightarrow 4f^7$ transitions intensity variation observed in the XEOL (Fig. 3). The weak emission intensity of Eu^{3+} 4f-4f transitions, since the Eu^{3+} species are more abundant than Eu^{2+} may be explained by the higher probability of Eu^{2+} transitions when compared to Eu^{3+} ions. The Eu^{2+} $4f^65d^1$-$4f^7$ transition is allowed by the Laporte's rule [22], and consequently presents shorter lifetime decay (ca. 1 μ) and is more probable than the Eu^{3+} 4f-4f transitions (several ms) which are allowed by magnetic dipole and force electric dipole [23].

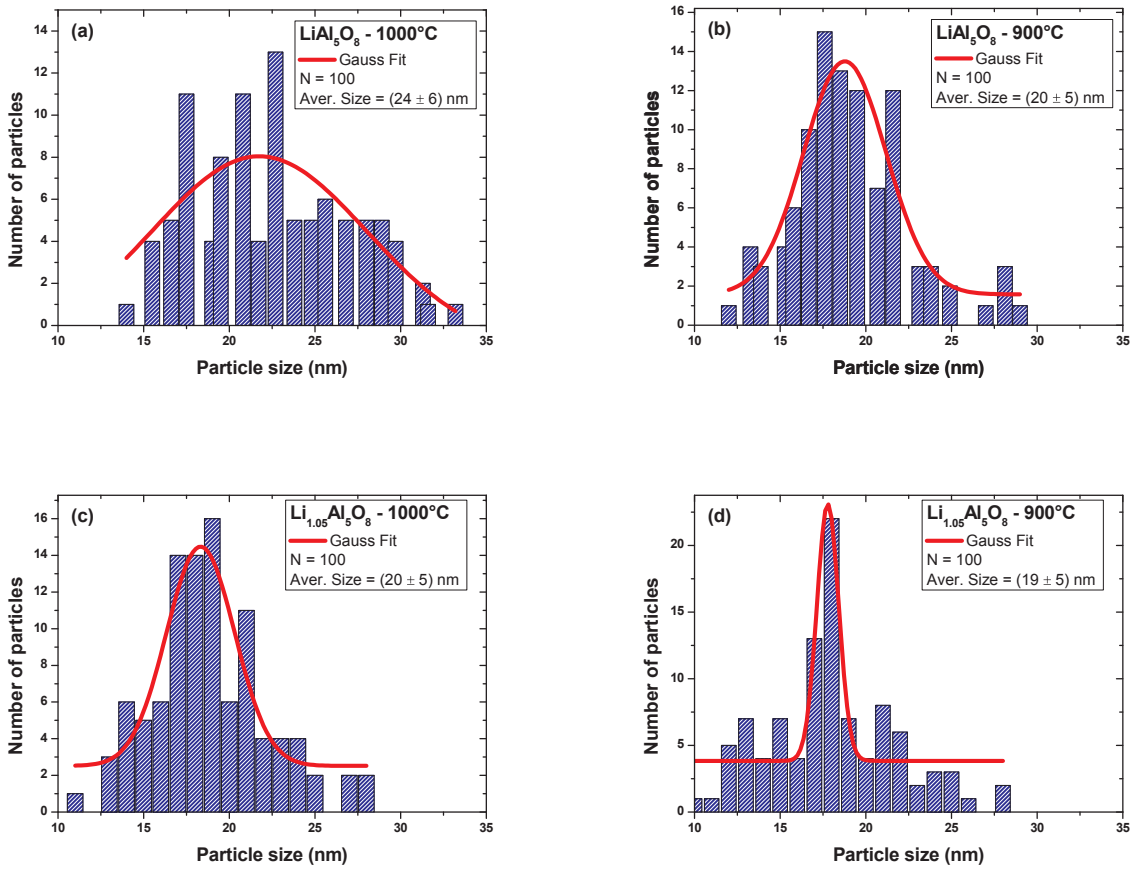

Fig. 2. Histograms calculated for (a) $LiAl_5O_8$ 1000 °C, (b) $LiAl_5O_8$ 900 °C, (c) $Li_{1.05}Al_5O_8$ 1000 °C and (d) $Li_{1.05}Al_5O_8$ 900 °C, considering a set of 100 dispersed nanoparticles.

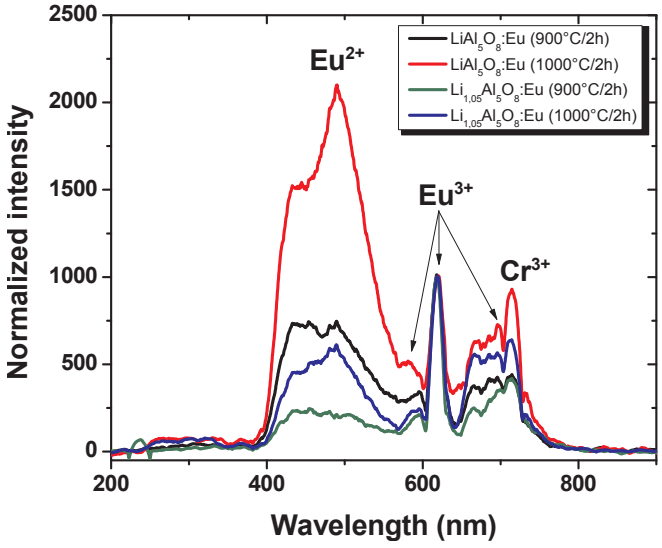

Fig. 3. Eu-doped $LiAl_5O_8$ and $Li_{1.05}Al_5O_8$, calcined at 900 and 1000 °C, emission spectra under excitation at the Eu-L_{III} edge.

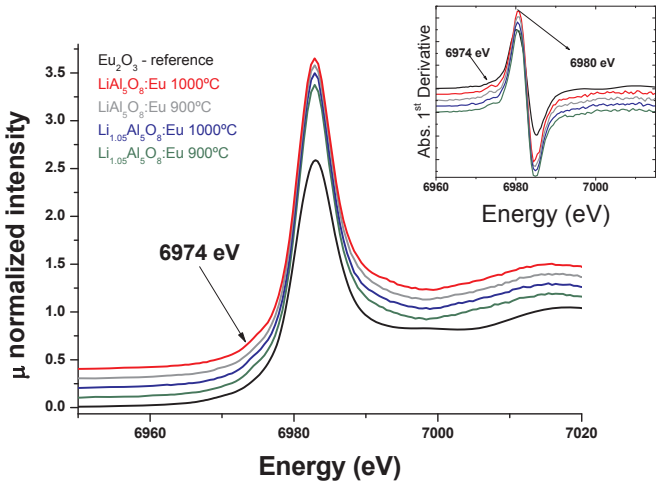

Fig. 4. XANES of Eu-doped $LiAl_5O_8$ and $Li_{1.05}Al_5O_8$ (calcined at 900 and 1000 °C) around the Eu-L_{III} edge.

4. Conclusion

In this work, Li^+ excess influence on the structural, morphologic and luminescent properties of the Eu-doped $LiAl_5O_8$, as well as the thermal treatment conditions were reported. The optical behavior was investigated through XEOL technique and the results suggested a mix of Eu^{2+} and Eu^{3+} valences for all samples, due to a broadband emission attributed to Eu^{2+} and sharp lines ascribed as Eu^{3+} transitions. Some transitions in the near-infrared assigned as Cr^{3+} transition were also observed in the XEOL emission spectra and it was ascribed to the chromium trace present in the starting reactants $Al(NO_3)_3$. XANES was used to investigate the Eu valence and the results indicated it is mainly in the trivalent form. By the XANES results, it was observed a small shoulder in the spectra at 6974 eV, suggesting the coexistence of Eu^{2+}, independent of the synthesis conditions. From the luminescence results, it is clear that the samples of $LiAl_5O_8$ present a higher amount of Eu^{2+} than the $Li_{1.05}Al_5O_8$ and the temperature also influences this tendency. Thus, in this work we demonstrated the influence of the thermal

treatment and the Li^+ self-doping on the Eu-doped $LiAl_5O_8$ and $Li_{1.05}Al_5O_8$ phosphors.

Acknowledgements

The authors are grateful to the FINEP (Brazilian Innovation Agency), CAPES (Brazilian Federal Agency), CNPq (No. 470.972/2013-0) (Brazilian National Council for Scientific and Technological Development). We thank the X-ray Absorption and Fluorescence Spectroscopy beamline (XAFS2) from the Brazilian Synchrotron Light Laboratory (LNLS) and Electron Microscopy Laboratory (LME) from the Brazilian Nanotechnology Laboratory (LNNano), both from the Brazilian Center for Research in Energy and Materials (CNPEM) for the facilities and the financial support. We are also thankful to Dr. A.P.S. Sotero, Dr. S.A. Figueroa and J.C. Maurício (XAFS2/LNLS) and Dr. Fabiano Montoro (LME/LNNano) for the assistance during the experiments.

References

[1] X. Li, G. Jiang, S. Zhou, X. Wei, Y. Chen, C.K. Duan, M. Yin, Sensor. Actuator. B Chem. 202 (2014) 1065–1069.
[2] U. Rambabu, T. Balaji, S. Buddhudu, Mater. Res. Bull. 30 (1995) 891–895.
[3] T. Jüstel, J.C. Krupa, D.U. Wiechert, J. Lumin. 93 (2001) 179–189.
[4] S. Zhang, G. Wu, C. Duan, J. Wang, J. Rare Earths 29 (2011) 737–740.
[5] D. Jin, J. Yang, X. Miao, L. Wang, L. Wang, Int. J. Appl. Ceram. Technol. 10 (2013) 603–609.
[6] W.-N. Wang, W. Widiyastuti, T. Ogi, I.W. Lenggoro, K. Okuyama, Chem. Mater. 19 (2007) 1723–1730.
[7] G. Bai, M.-K. Tsang, J. Hao, Adv. Opt. Mater. 3 (2015) 431–462.
[8] T. Takeda, D. Koshiba, S. Kikkawa, J. Alloys Compd. (2006) 879–882.
[9] O.A. Lopez, J. McKittrick, L.E. Shea, J. Lumin. 71 (1997) 1–11.
[10] V.C. Teixeira, L.C.V. Rodrigues, D. Galante, M.V. dos S. Rezende, Opt. Mater. Express 6 (2016) 2871.
[11] S.J.A. Figueroa, J.C. Mauricio, J. Murari, D.B. Beniz, J.R. Piton, H.H. Slepicka, M.F. de Sousa, A.M. Espíndola, A.P.S. Levinsky, J. Phys. Conf. Ser. 712 (2016) 012022.
[12] D.A. Hora, A.B. Andrade, N.S. Ferreira, V.C. Teixeira, M. V. dos S. Rezende, Opt. Mater. 60 (2016) 495–500.
[13] G.A. Sobral, M.A. Gomes, J.F.M. Avila, J.J. Rodrigues, Z.S. Macedo, J.M. Hickmann, M.A.R.C. Alencar, J. Phys. Chem. Solid. 98 (2016) 81–90.
[14] A.E. Danks, S.R. Hall, Z. Schnepp, Mater. Horizons 3 (2016) 91–112.
[15] J. Schindelin, C.T. Rueden, M.C. Hiner, K.W. Eliceiri, Mol. Reprod. Dev. 82 (2015) 518–529.
[16] Z.L. Wang, X. Feng, J. Phys. Chem. B 107 (2003) 13563–13566.
[17] A.P. Jadhav, A. Pawar, U. Pal, B.K. Kim, Y.S. Kang, Sci. Adv. Mater. 4 (2012) 597–603.
[18] V. Singh, T.K. Gundu Rao, J. Solid State Chem. 181 (2008) 1387–1392.
[19] V.C. Teixeira, P.J.R. Montes, M.E.G. Valerio, Opt. Mater. 36 (2014) 1580–1590.
[20] P.J.R. Montes, M.E.G. Valerio, J. Lumin. 130 (2010) 1525–1530.
[21] P.J.R. Montes, V.C. Teixeira, D.A.B. Barbosa, C.W.A. Paschoal, M.V. dos S. Rezende, J. Alloys Compd. 708 (2017) 79–83.
[22] K. Binnemans, Coord. Chem. Rev. 295 (2015) 1–45.
[23] O.L. Malta, L.D. Carlos, Quim. Nova 26 (2003) 889–895.